Workshop IV

Astrophysical Maser Radiation

Introduction:

- orientation in the observations
- basic physics considerations
  - ordinary radiative transfer eqns. are applicable
  - creating an inversion (calculation vs "phenom...")
  - degree of saturation (R/R'), critical role (uncertain due to beaming angle)
  - exponential vs linear gain
  - spectral line narrowing + rebroadening

Research Issues:

- Calculation of masing in Keplerian disks.
  - identifying + interpreting accretion disks
- Calculation of polarization in maser radiation, and implications for magnetic fields.
  - MHD turbulence
  - inferring B from Stokes V (Zeeman vs "non-Zeeman")

General Orientation about masers in astronomy.

brightness temperatures up to $\simeq 10^{15}$ K
(that's how we know they are masers)

sizes down to 10^{13} cm or less

reveal structure at the smallest spatial scales, using radio interferometers (VLBA, etc).

physical conditions $T_{gas} \simeq 100-1000$
density (hydrogen) $\simeq 10^{6}-10^{10}$ cm^{-3}

astronomical environments
- circumstellar – late-type giants / supergiants
- interstellar – star-forming regions, SN shocks
- nuclei of active / middle active galaxies.

molecular species – OH, H_2O, SiO, CH_3OH

frequencies – 1–500 GHz

initial detections – 1960's.

nature

INTERNATIONAL WEEKLY JOURNAL OF SCIENCE

Volume 373 No. 6510 12 January 1995 $8.50

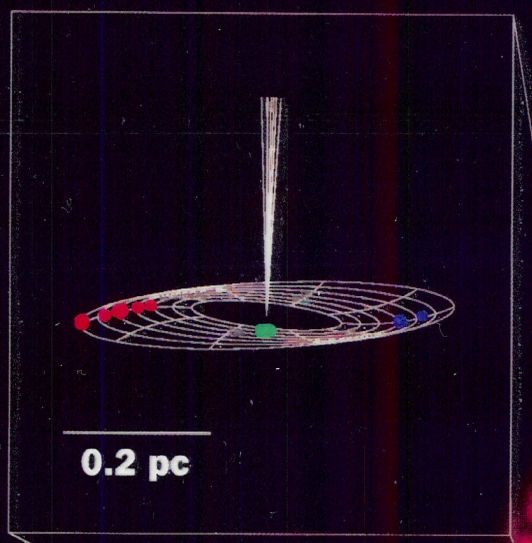

2,000 pc

Zooming in on a black hole

Dynamics of HIV-1 infection

The Pope and embryology

Multi-ring impact basins

Why maser radiation?

— high brightness temperatures ($\gtrsim 10^{10}$ K)
[molecules destroyed at such thermal temp]
[+ narrow spectral lines]

Masers are highly beamed
(+ elongated or "tubular")

— pumping + "thermodynamic limit"
— brightness temperature
+ inferred $\int$(intensity) $d\Omega$ from saturation
— strongest rays deplete population inversion

=> simple picture

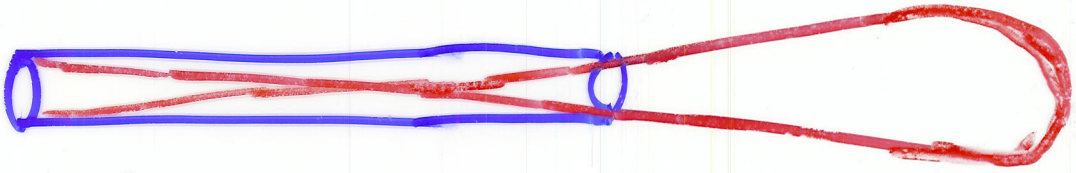

bidirectional or not

$$\frac{\text{diameter}}{\text{length}} \lesssim 0.1$$

- though small,
  beaming angle >> Fresnel angle
  (=> incoherent radiation)

- spectral linebreadth >> molecular state lifetime
  (no "multiphoton effects")

- single traversal (no "mirrors")

- no instabilities

* => use ordinary, time independent radiative transfer eqns. (but with negative opacities).

* commonly, approximate maser as linear to get simple solutions

How might inversion of the molecular populations occur?

(simple 3-level model).

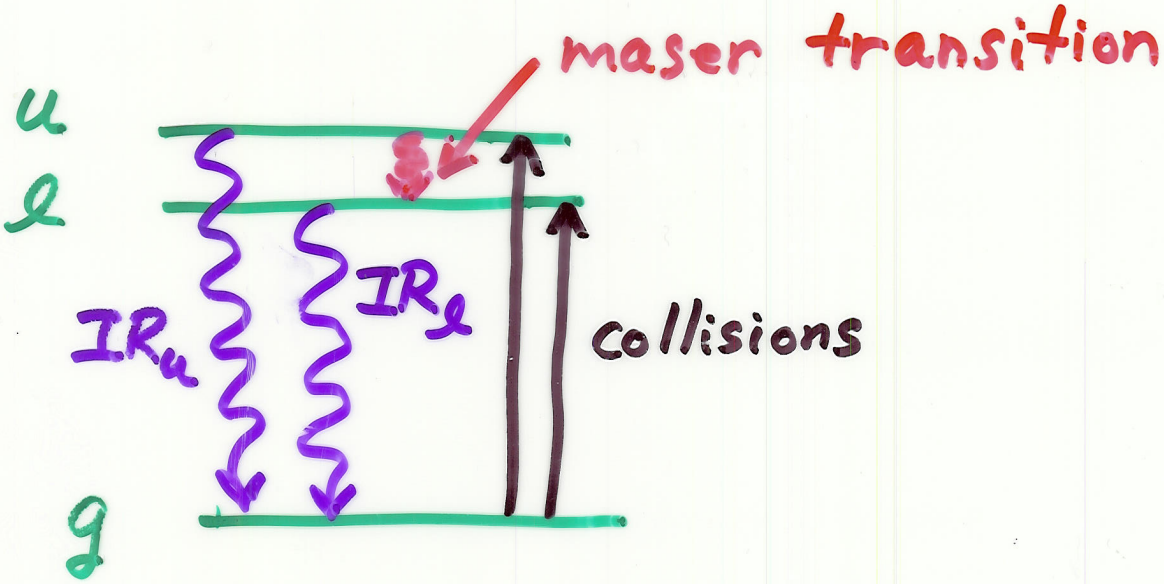

collisions aren't ordinarily selective

but, rate (IR_l) > rate (IR_u)

is possible and then causes

$n_u > n_l$ (inversion).

[note: IR radiation must escape.
Large optical depths for IR
"quench" the population inversion!

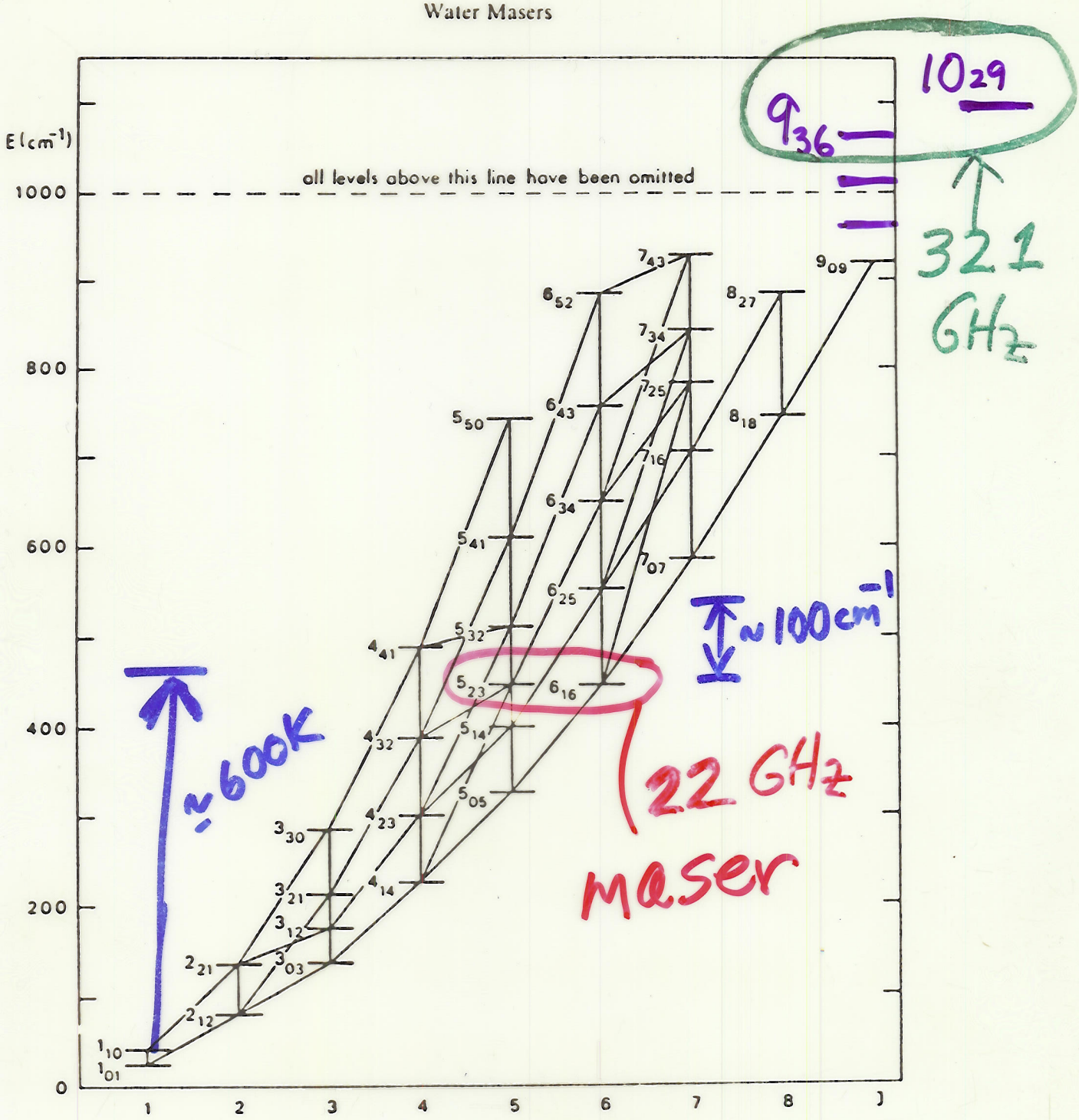

l rotational energy levels of water below 1000 cm^{-1} for which K_{-1}, K_{+1} = odd, even or even, odd. Electric dipole-allowed transitio
ΔK_{-1}, $\Delta K_{+1} = \pm 1, \pm 1$, are indicated by lines connecting the levels

nost exclusively restricted to the next lower
ne level while the other levels have more than
rong downward transition available plus a
of weaker transitions (see Table 2). Conse-
under non-LTE conditions population tends
up along the backbone (hence the name). The
vo downward transitions by which population
: removed from the backbone ladder are the

difference is not washed out by transitions in the lin
The populations of the upper and lower level are the
determined independently by transitions to other leve
Secondly, for the same reason collisional coupling of th
upper and lower level must be small. This requir
either a small cross section ($\sigma_{ij} \lesssim 10^{-16}$ cm^2) f
collisional transitions over the line or a relative
low particle density ($n_{H_2} \lesssim 10^9$ cm^{-3}). Thirdly, the leve

2-Level, Linear Maser

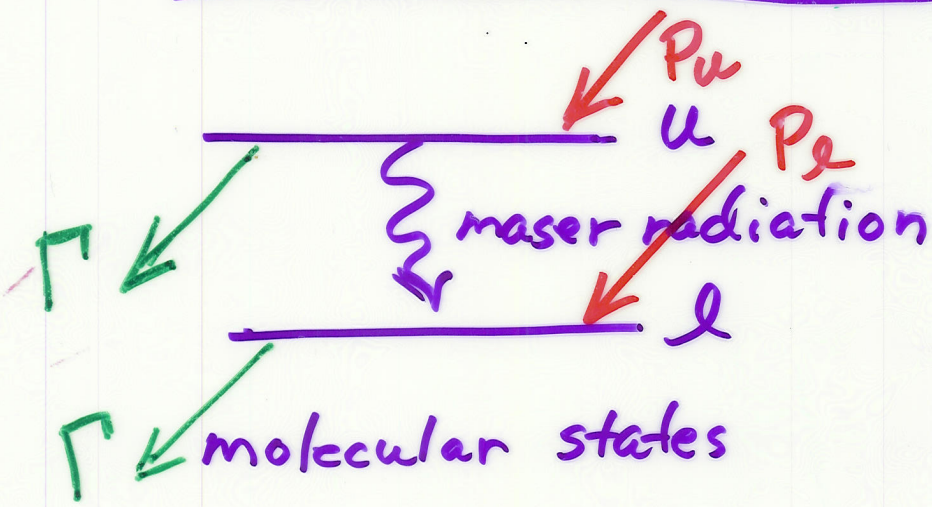

eqn. of rad. trans.

linear maser

$$\frac{dI}{ds} = \left(\frac{h\nu}{4\pi\Delta\nu}\right)\left[(n_u - n_\ell)BI + \text{spontaneous emission}\right]$$

populations per substate

Einstein "B coefficient"

ignore

(A) "UNSATURATED" – I not influence populations

$n_u - n_\ell \neq f(I)$

$\Rightarrow dI/ds = L^{-1}I \Rightarrow I = I_0 e^{s/L}$ "exponential gain"

(B) "SATURATED" – I (through stimulated emission) dominates decay of $(n_u - n_\ell)$

$\Rightarrow (n_u - n_\ell) \propto 1/I \Rightarrow dI/ds = \text{constant } C$

$\Rightarrow I = Cs + \cancel{I_0}$ "linear gain"

Spectral line narrowing / rebroadening.

$$\Delta P(v) \propto e^{-mv^2/2kT} \quad \text{(Maxwellian)}.$$

with Doppler relation $V_v = (\nu - \nu_0)\, c/\nu_0$

$$\Delta P(V_v) \propto e^{-(\nu-\nu_0)^2/\nu_D^2}$$

- Unsaturated limit

$$I(\nu) = I_0\, e^{(\ldots)s} = I_0 \exp\left[K_0 s\, e^{-(\nu-\nu_0)^2/\nu_D^2}\right]$$

for large $K_0 s$, this distribution has a half-breadth

$$\Delta\nu_{1/2} = (\nu-\nu_0)_{1/2} \simeq \nu_D \left(\frac{\ln 2}{K_0 s}\right)^{1/2}$$

can be $\simeq \nu_D/5$ (line narrowing).

- saturated limit

$$I(\nu) = (hc\,\Delta P/2)\, s\, e^{-(\nu-\nu_0)^2/\nu_D^2}$$

$$= \text{constant} \times s \times e^{-(\nu-\nu_0)^2/\nu_D^2}$$

same line profile as Maxwellian of the gas (rebroadening).

δ = normalized mean square deviation from Gaussian fit.

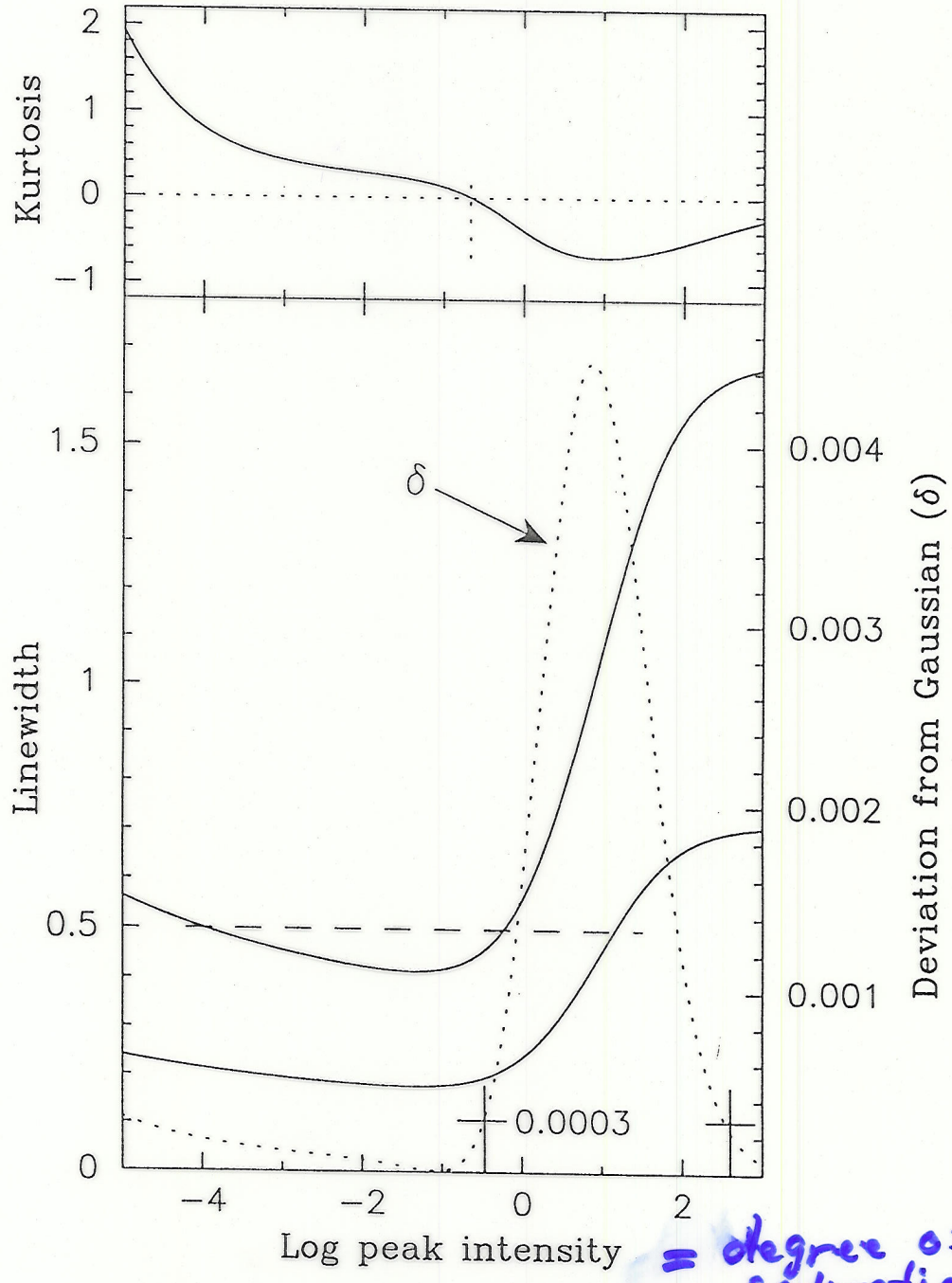

= degree of saturation (here)

FIG. 2.—*Lower panel*: Representative line widths $\Delta v_{1/2}$ (arbitrary units), calculated as a function of the log of the peak intensity I_p for masing gas at two gas temperatures. The horizontal line at $\Delta v_{1/2} = 0.5$ represents an observed line width. Its intersections with the curves for the calculated line widths determine the gas temperatures and intensities that are compatible with this line width. Deviation of the profile from a Gaussian as measured by δ is given by the dotted curve on which the crosses mark $\delta = 3 \times 10^{-4}$ that is representative for the observed profiles in Fig. 1. Although the results of calculations are presented in this figure for only $I_c = 10^{-9}$, they are indicative for the range

FIG. 3.
yield a s
for Fig.
($\Delta v_{1/2}/0.5$
where M
are comp

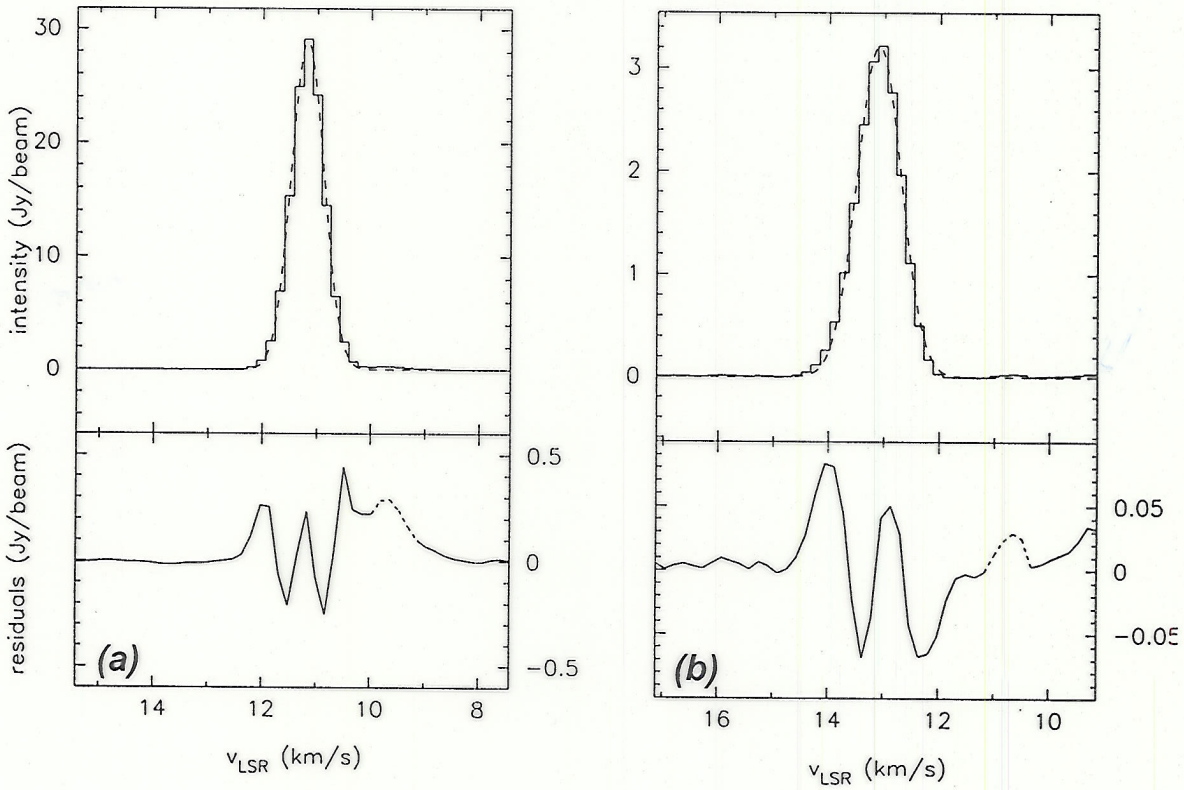

Fig. 12.— Best-fit Gaussians and fit residuals for the MERLIN profiles of the *(a)* F39A and *(b)* E24 masers. The portions of the residuals plotted using a dotted line are due to imaging artifacts in off-peak channels which are not included in the fitting or in the analysis.

OH 18 cm satellite lines (supernova shell)
Hoffman et al.

2-level transition without redistribution

$$\frac{dI(r,\hat{k},\nu)}{ds} = K(r,\hat{k},\nu)\, I(r,\hat{k},\nu) + \eta_s \exp(-\nu^2)$$

$$K(r,\hat{k},\nu) = \frac{1}{\pi}\int \frac{\exp(-w^2)\,\delta(\nu - \hat{k}\cdot\bar{w})}{1 + \bar{J}(r,\bar{w})}\, d\bar{w}$$

$$\bar{J}(r,\bar{w}) = \int I\left(r,\hat{k},\nu=\nu_0\left(1+\frac{\hat{k}\cdot\bar{w}}{c}\right)\right)\frac{d\hat{k}}{4\pi}$$

w = molecular velocity, normalized.

radial symmetry; $I, K, J = \text{fct}(|\vec{r}|)$

application thin disks, spheres.

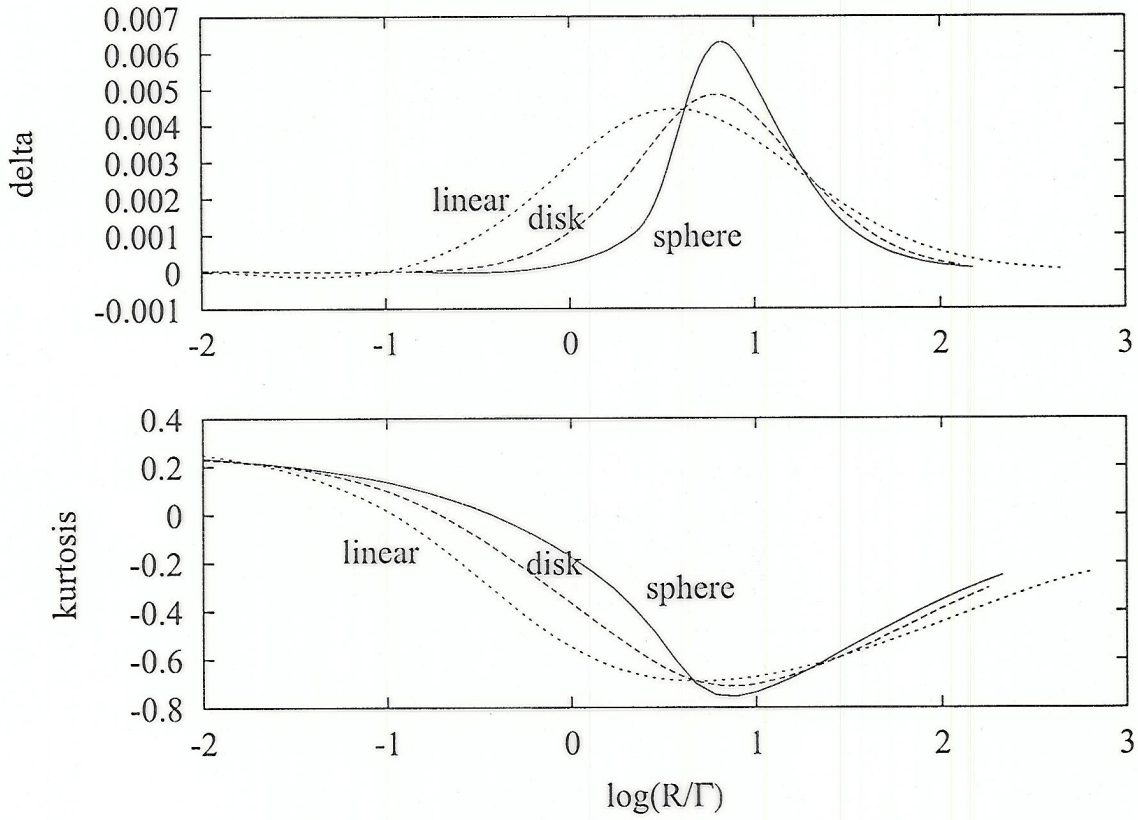

Fig. 2.— (upper panel) The quantity δ which measures the deviation of the profile of the radiation from the Gaussian that best fits the profile, as a function of the log of the degree of saturation, for the linear, thin (edge-on) disk and spherical masers (with $\widetilde{I}_0 = 10^{-9}$). (lower panel) The kurtosis K for the same profiles.

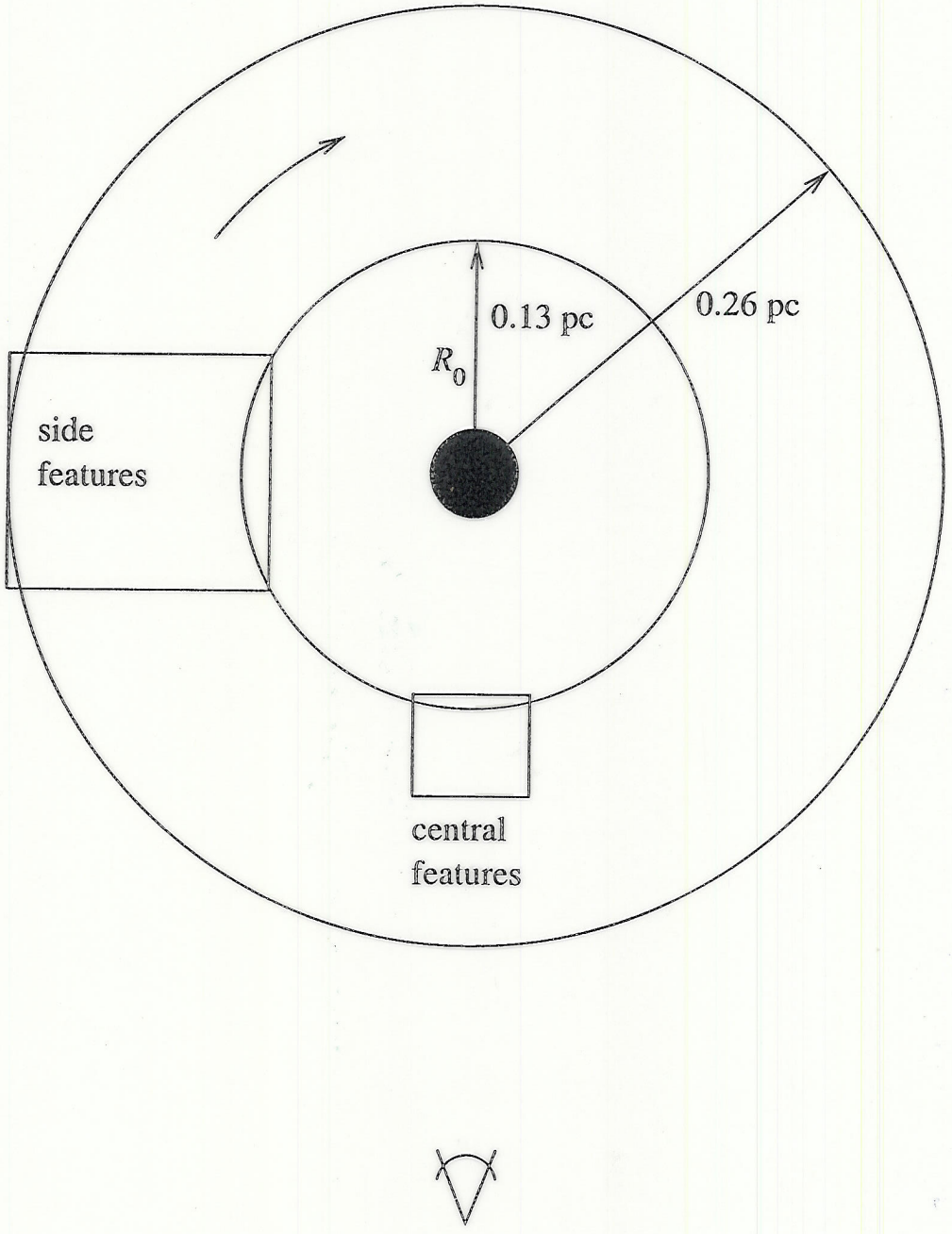
0.13 pc
0.26 pc
R_0
side
features
central
features

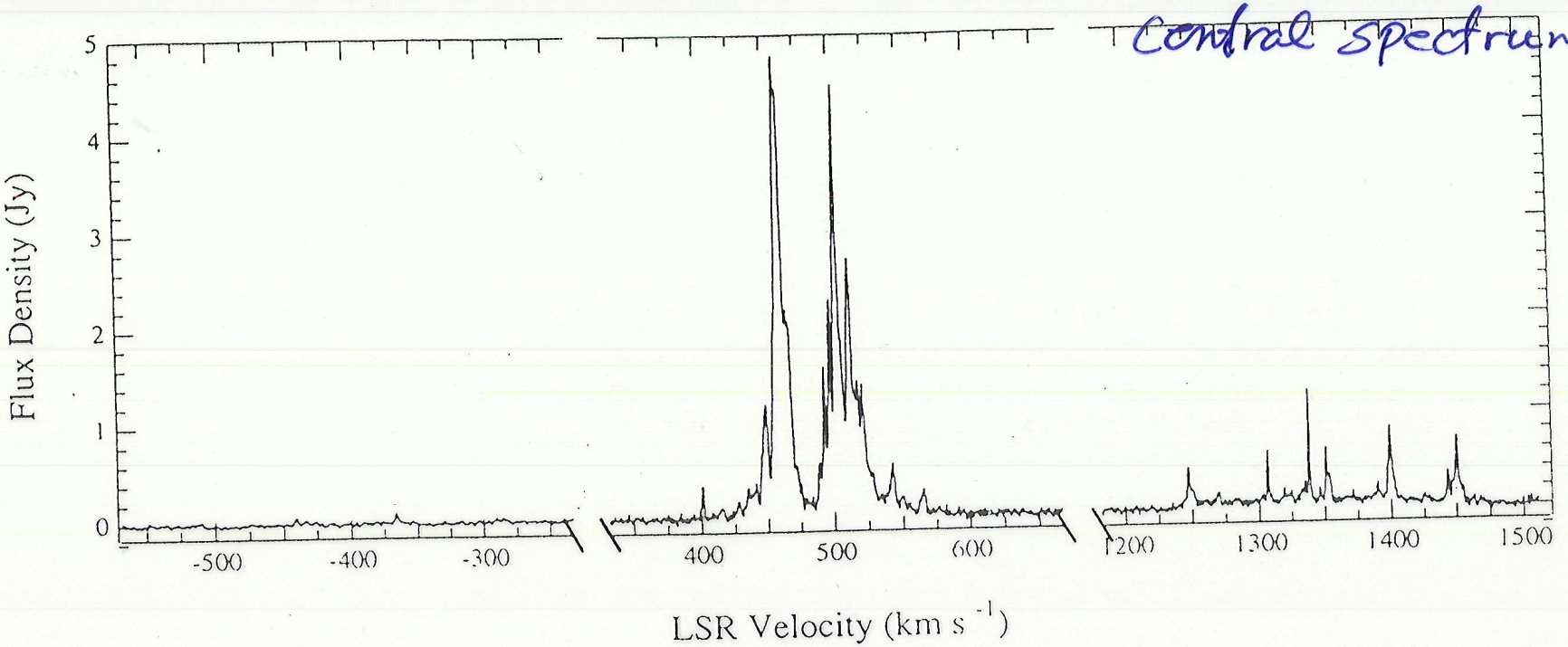

Fig. 1. H_2O megamaser emission associated with the nucleus of NGC 4258 on 1993 February 13. Shown are the 'low-velocity' components at about 500 km s^{-1} and the 'high-velocity' components at about −400 and 1350 km s^{-1}. Note that the velocity axis is compressed so as to omit velocities for which no emission was detected by Nakai et al. (1993). The channel spacing for the spectrum is 0.66 km s^{-1}. The flux calibrations for each of the three contributing spectra are uncertain by <30%. The conversion to heliocentric velocity is $V_{hel} = V_{LSR} - 8.2$ km s^{-1}. The radio definition of Doppler shift is assumed here and throughout.

2.2. *Search for new extragalactic masers*

In 1993 February we surveyed the nuclear regions of galaxies that have 100 μm flux densities greater than 20 Jy, and galaxies known to have compact nuclear structure, as well as selected fields in M 31 and M 101. Nuclei were surveyed for megamaser emission and H II complexes in the latter two galaxies were surveyed for emission similar to that associated with galactic star forming regions. The goal of the survey was to expand the number of candidates for VLBI observation (i.e., stronger than about 1 Jy in a 1 km s^{-1} line). With the 100-m Effelsberg antenna we observed 296 fields in 42 galaxies for 99 hours (Table 1). We omitted nuclei previously observed by Henkel et al. (1984) and prominent H II complexes NGC 5471, NGC 5462, NGC 5461, NGC 5455, and NGC 5447, Goss 1 (Israel et al. 1975), and H 47 (Hodge 1969).

3. Results

Our sample 100-m H_2O maser spectrum displayed in Fig. 1 shows the typical characteristics of both low and high-velocity emission. There are a great many maser lines blended to form the low-velocity complex. These were found to be highly time variable, with substantial fluctuations on time scales of weeks. One light-week corresponds to an angular size of ~ 0.190 milliarcseconds (mas), or 0.0059 pc, which is compara-

Wallin, Watson Wyld

central features
turbulent gas, unsaturated masers

flux

S/S_c

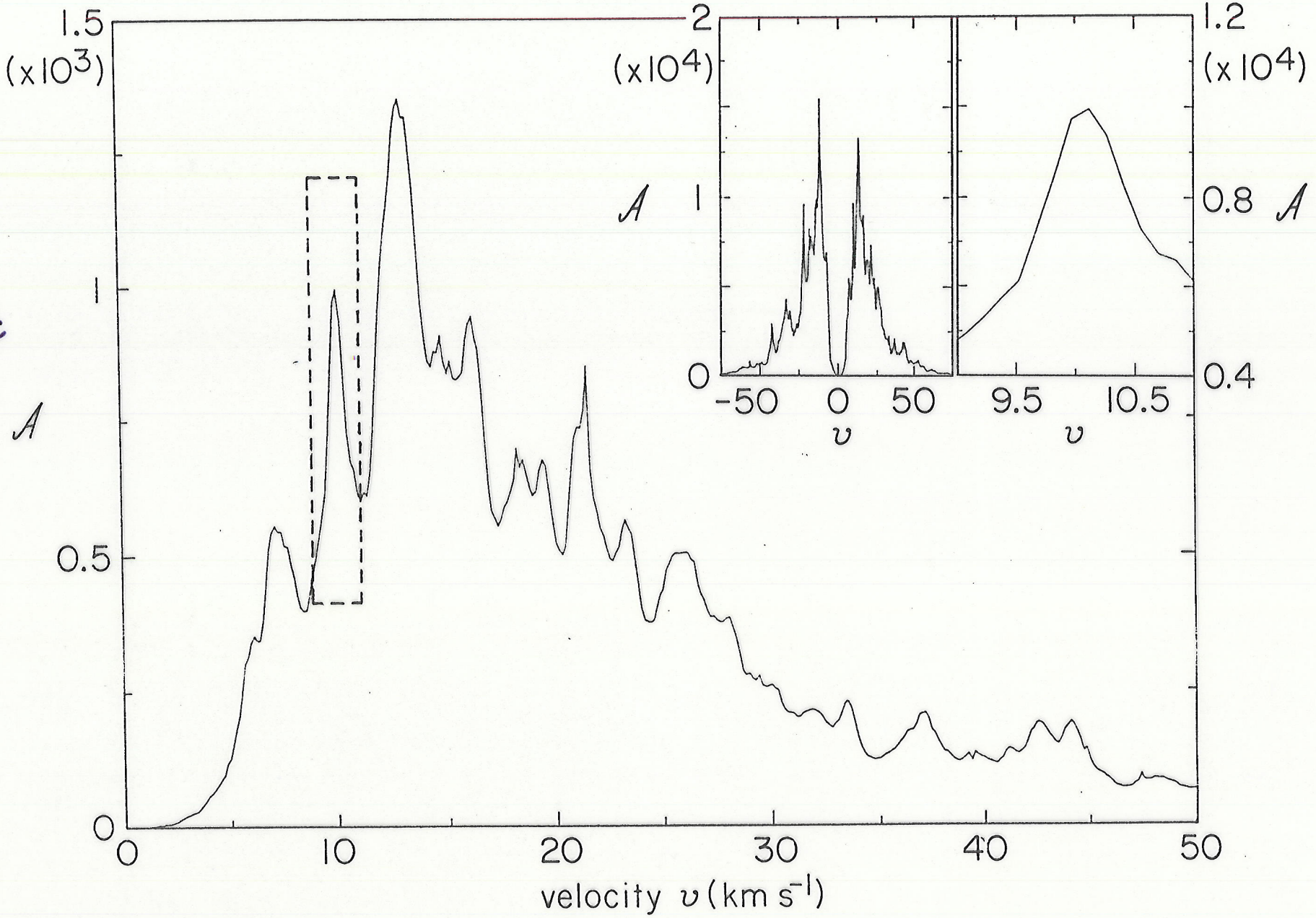

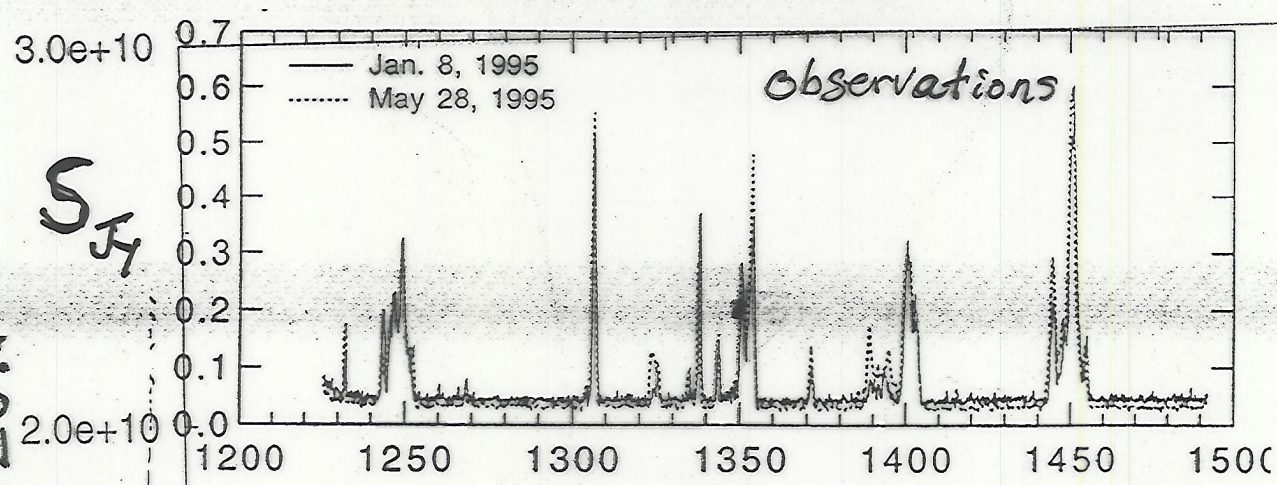

BELOW. A representative spectrum calculated for the emission from the side of the disk where it occurs at high velocities.

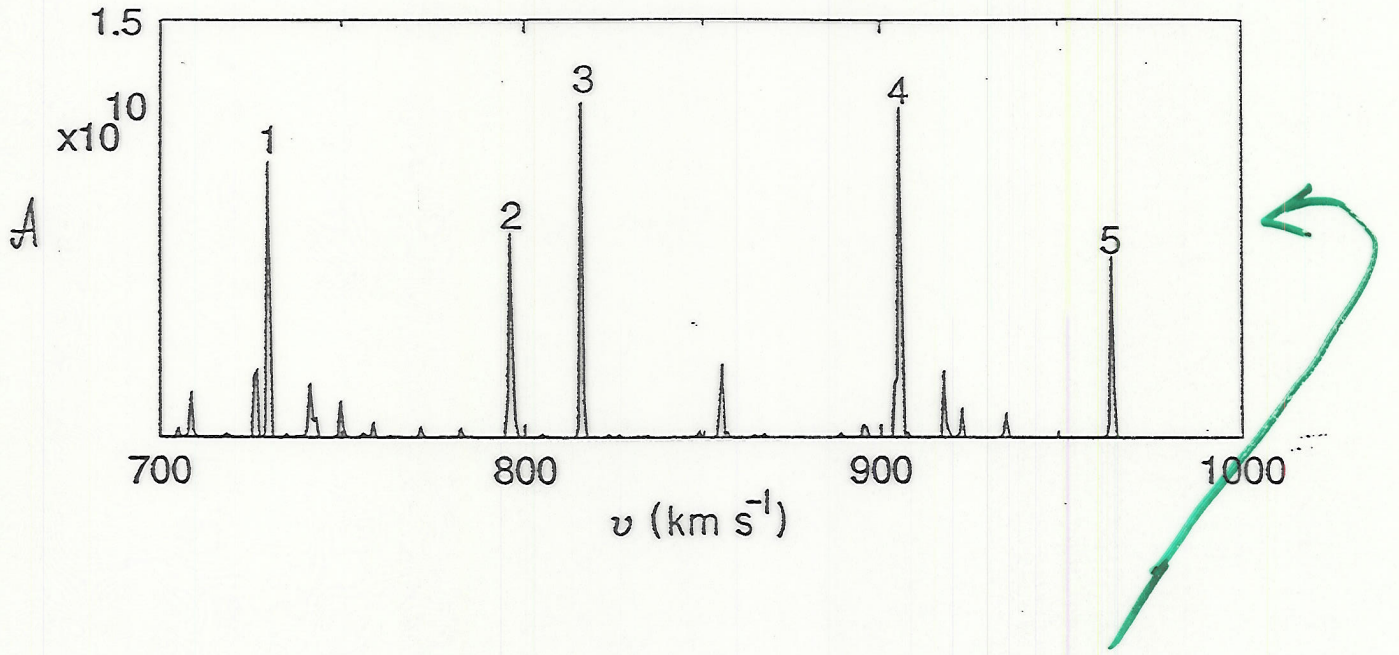

this galaxy
proximately
xies[4,20]. The
ver Neufeld
ucleus could
lded region
inversion of

lisk is offset
ating). Such

cosmic distance scale.

high rotation velocities in a sub-parsec region of NGC4258

Makoto Miyoshi*, James Moran†, James Herrnstein†, Lincoln Greenhill†, Naomasa Nakai‡, Philip Diamond§ & Makoto Inoue‡

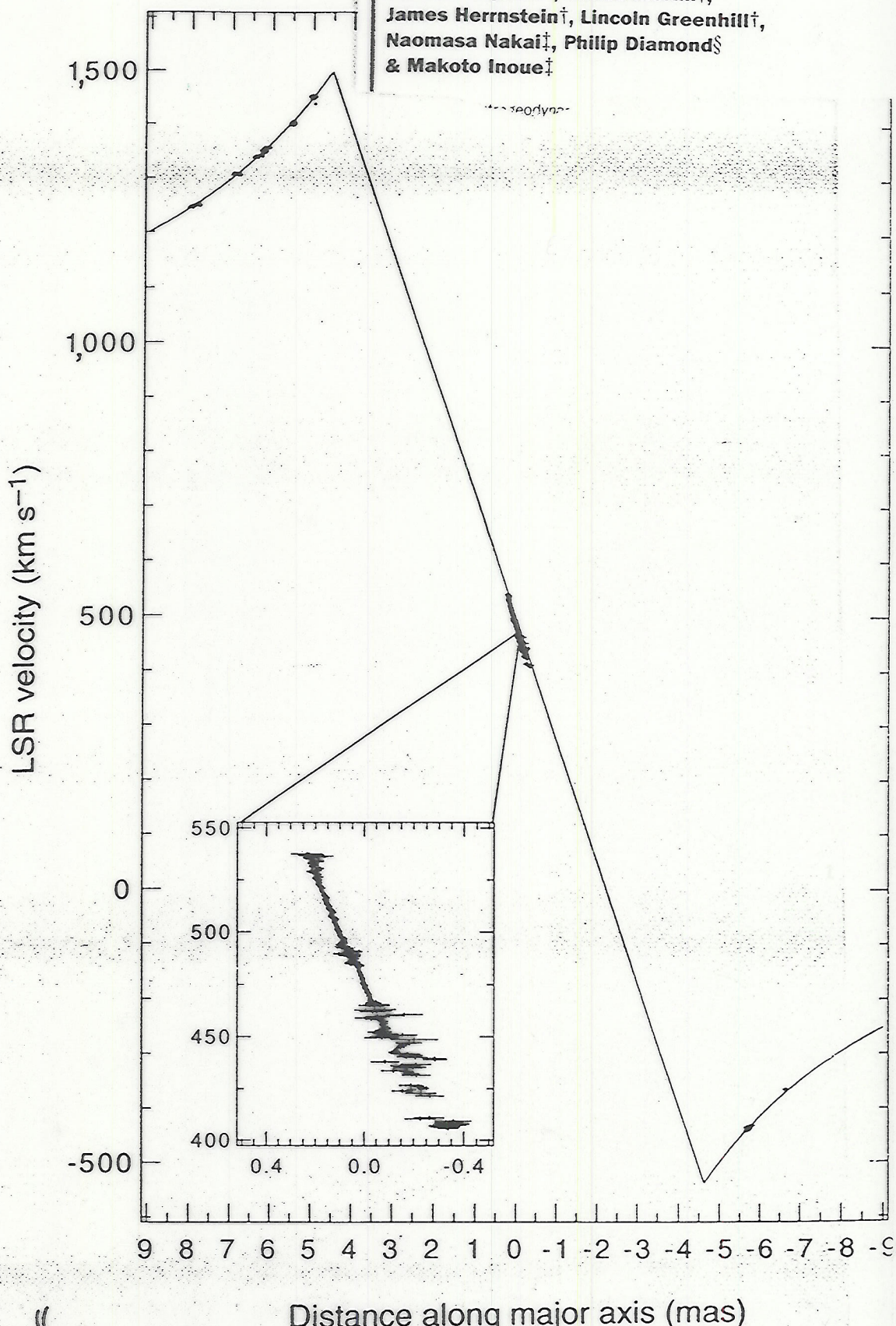

("along a line across the sky")

h) direction
calculated

FIG. 3 Line-of-sight velocity versus distance along the major axis (
tion angle, 86°). Inset, data near the systemic velocity of the ga
The position

Contours of constant intensity

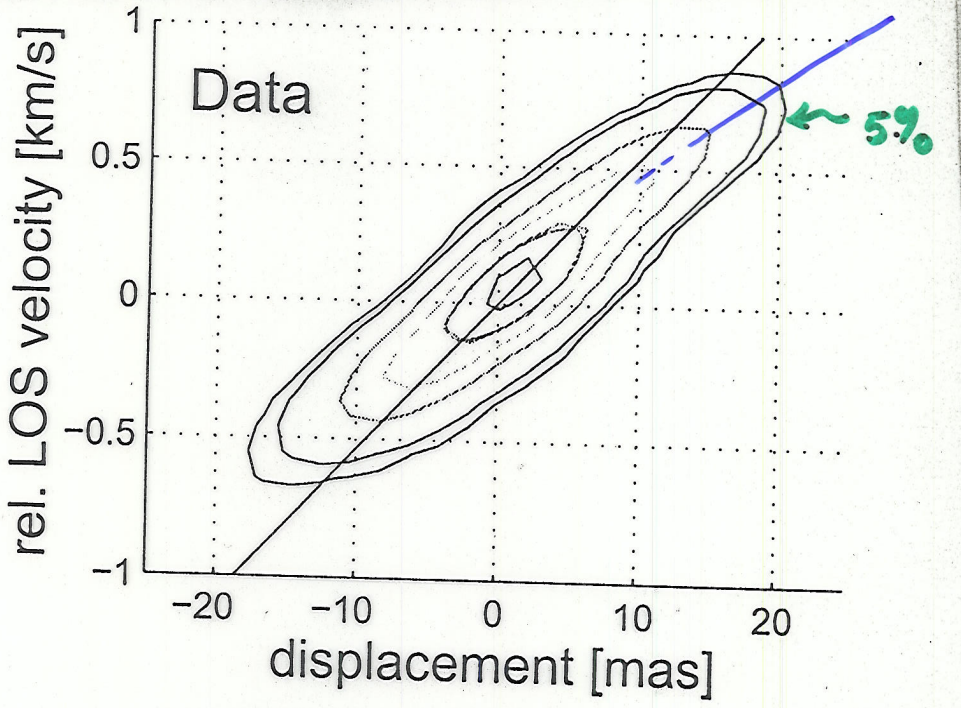

Fig. 4.— Same as figure 3 for the 6.7 GHz maser.

(methanol)

Pestalozzi et al.

Polarization of Astrophysical Masers

(to gain information about magnetic field)

convenient regimes —

- Zeeman splitting >> linebreadth
  (strong OH masers)
- Zeeman splitting << linebreadth
  (essentially all others)

Key consideration:

Zeeman frequency (ν_z) vs molecular state lifetime

if $2\pi\nu_z >>$ lifetime, greatly simplified!

(likely holds; e.g.
for SiO masers + B = 0.1G
$2\pi\nu_z \simeq 10 \times$ lifetime)

then only ordinary populations of magnetic substates enter (off diagonal density matrix elements = 0)

---

most (not all) studies for J=1-0 (or 2-1) transition of linear masers assumed to be representative.

● Zeeman splitting ν_Z >> linebreadth $\Delta\nu$

OH (ground state, 1.7 GHz)

characteristic: absence of Zeeman π components of Zeeman triplet.

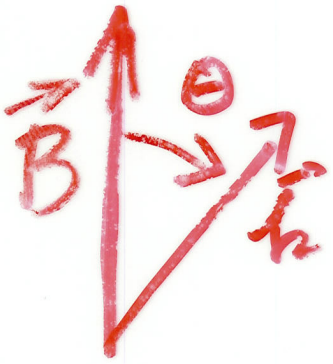

in an isotropic medium, optical depths for $\pi(\Delta M=0)$ (linear) and $\sigma(\Delta M=\pm 1)$ (elliptical)

$\tau_\sigma = \tau_0 \frac{1}{2}(1+\cos^2\theta)$, mostly $\parallel B$

$\tau_\pi = \tau_0 \sin^2\theta$, mostly $\perp B$

MHD turbulence (Goldreich-Sridhar), is anisotropic and creates a preference for optical depths $\parallel B$,

$$\sqrt{\left\langle \frac{\partial v_s}{\partial s} \right\rangle_\perp} > \left\langle \frac{\partial v_s}{\partial s} \right\rangle_\parallel \Rightarrow |\tau_{0\parallel}| > |\tau_{0\perp}|$$

molecular velocity

=> stronger masing $\parallel$ to B (σ's) than $\perp$ to B (π's), but how much? (numerical).

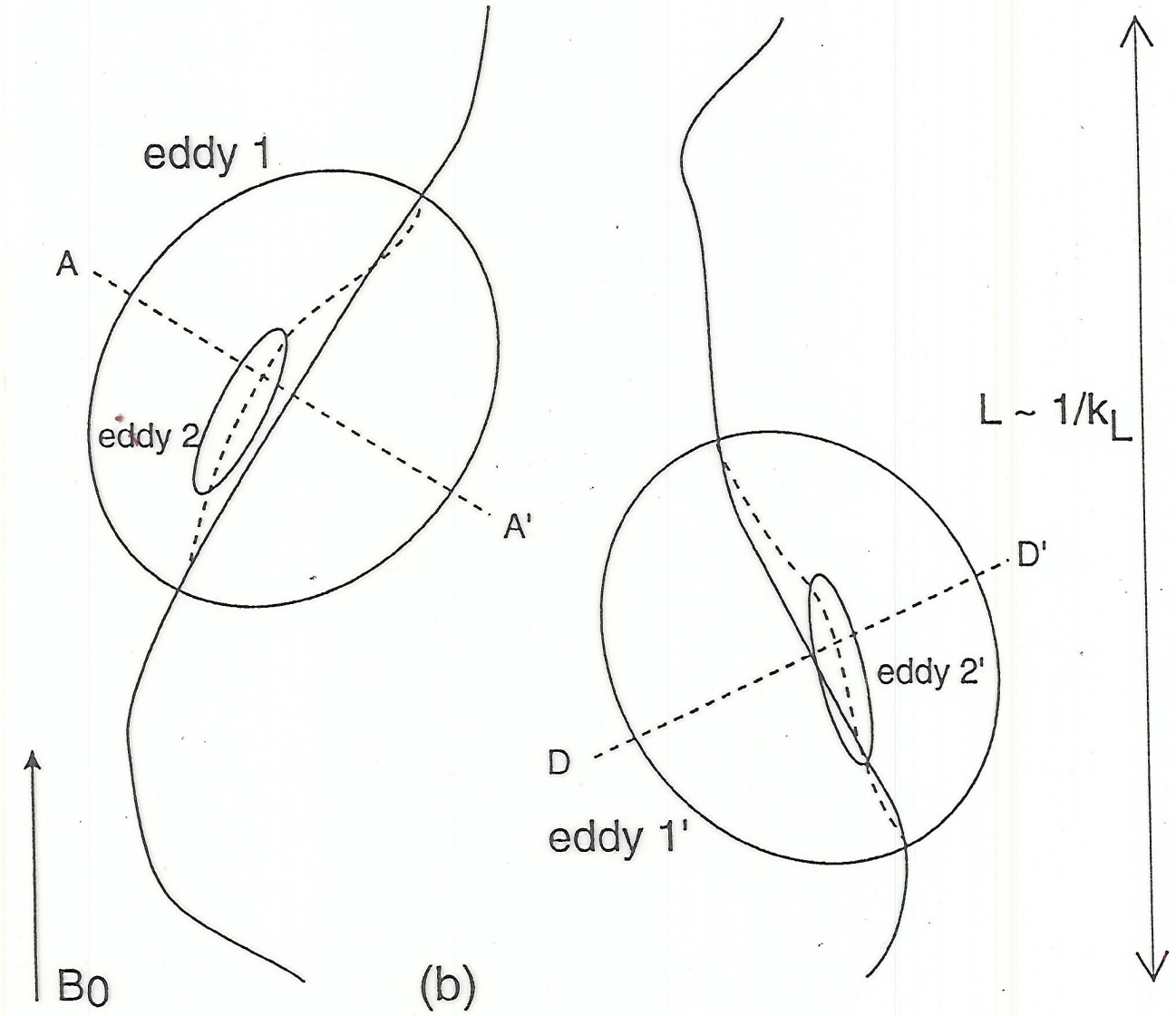

MHD turbulence

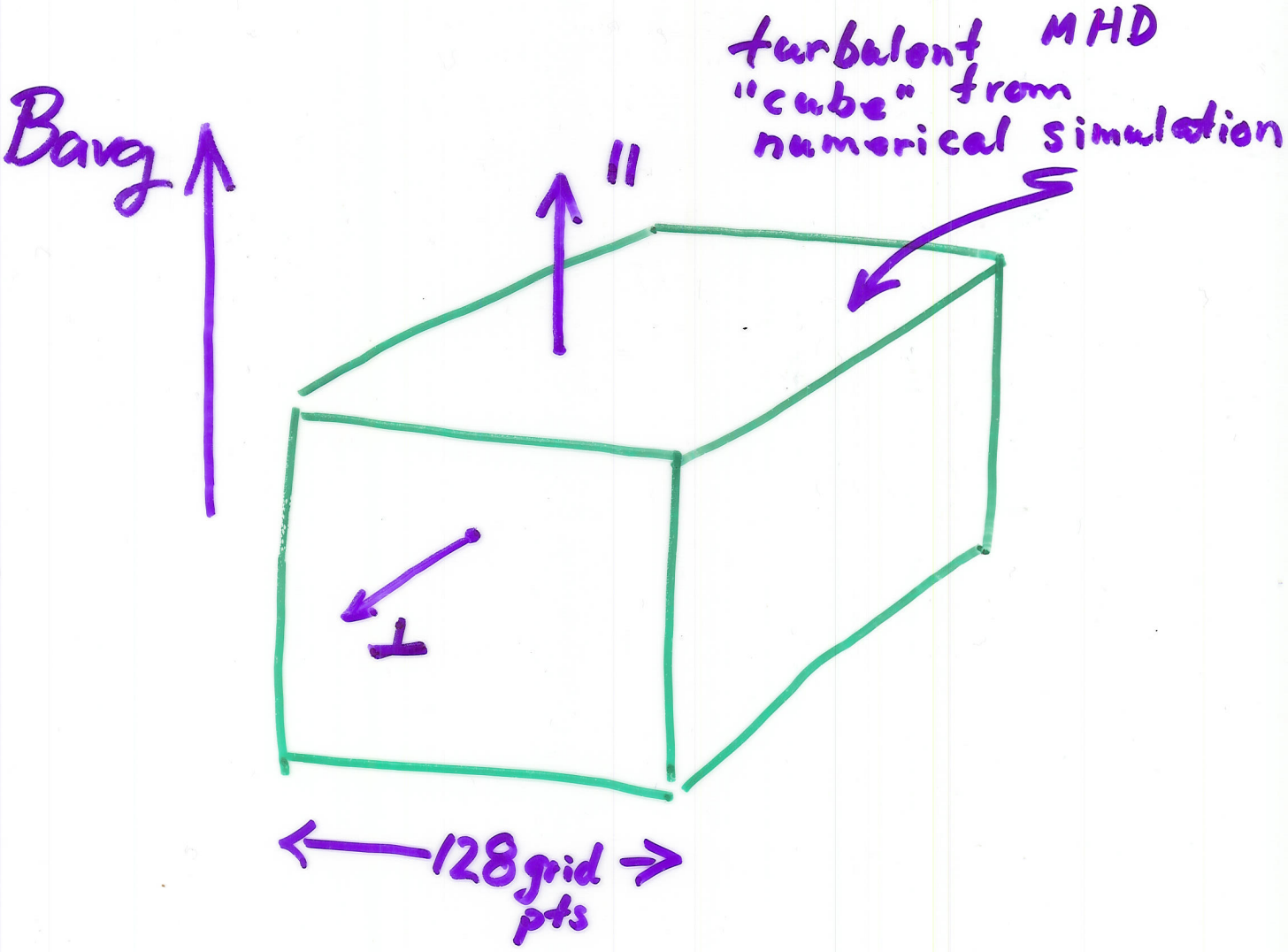

compute histogram of optical depths of $(128)^2$ rays from face for $\tau_\perp$ and $\tau_\parallel$.

for maser radiation.

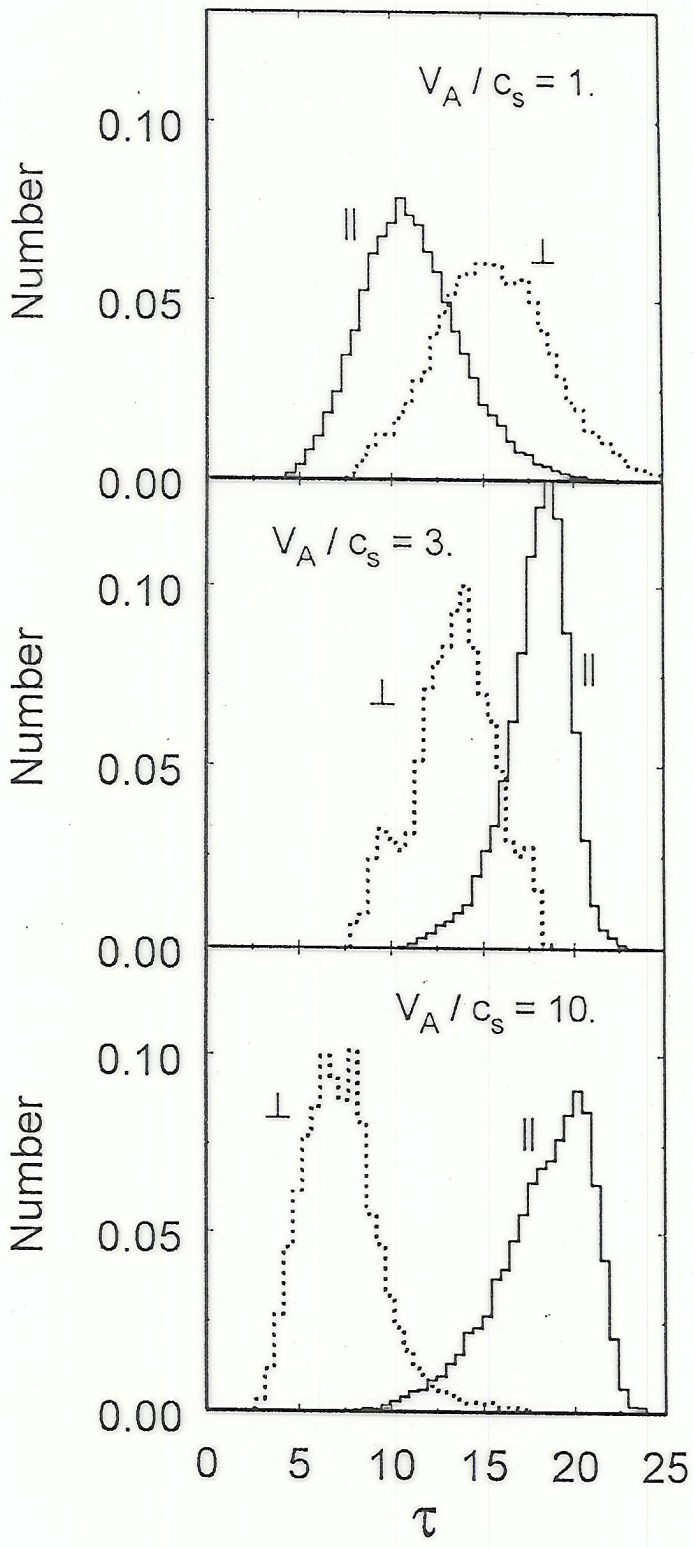

FIG. 1.—Representative histograms for the number of rays with unsaturated optical depths τ. The optical depth is obtained at the peak intensity of each ray. The numbers are given as a fraction of the 128^2 rays from the surface of a turbulent cube within intervals of 0.5 in τ. Separate histograms (as indicated) are shown for rays that propagate parallel and perpendicular to the average magnetic field of the turbulent cube for the three choices $v_A/c_s = 1$, 3, and 10.

Watson, Wicker, Gammie & McKinney

$$\frac{d}{ds}\begin{pmatrix} I \\ Q \\ U \\ V \end{pmatrix} = \begin{pmatrix} A & B & 0 & C \\ B & A & 0 & 0 \\ 0 & 0 & A & 0 \\ C & 0 & 0 & A \end{pmatrix}\begin{pmatrix} I \\ Q \\ U \\ V \end{pmatrix}$$

in frame of local magnetic field.

$J=1-0$ transition

$$A = (1+\cos^2\theta)(n_+ + n_-) + 2n_0 \sin^2\theta$$

$$B = \sin^2\theta\,(n_+ + n_- - 2n_0)$$

$$C = 2\cos\theta\,(n_+ - n_-)$$

population differences $n_{\pm,0}(\vec{r}, v_{\pm,0})$
evaluated at velocities $v_{\pm,0}$ from

$$(1 - v_{\pm}/c)\,\nu = \nu_0 \pm \nu_Z$$

and $(1 - v_0/c)\,\nu = \nu_0$

in unsaturated limit

n's & Gaussians.

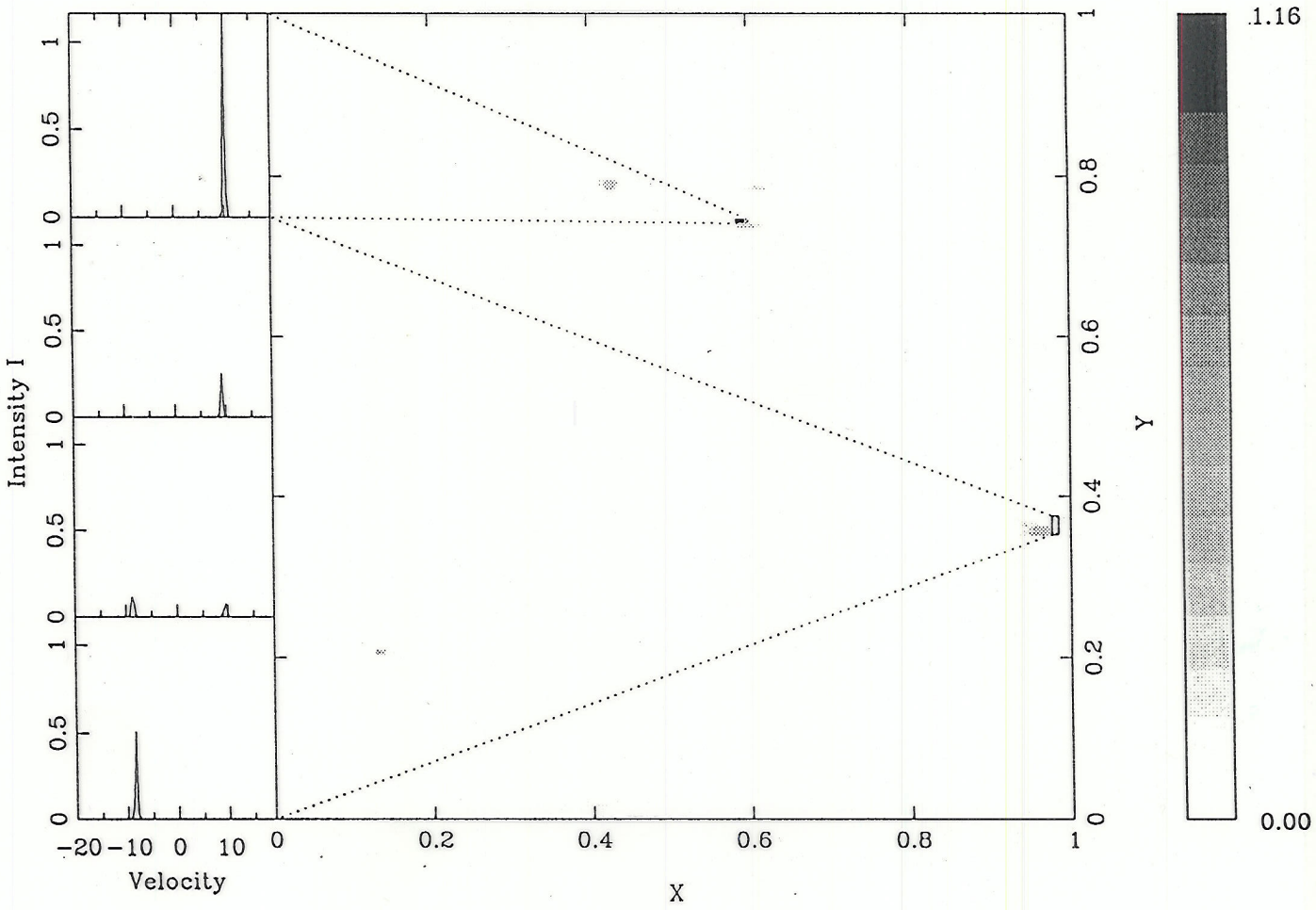
Intensity I
0
0.5
1
0
0.5
1
0
0.5
1
0
0.5
1
−20 −10 0 10
Velocity
0 0.2 0.4 0.6 0.8 1
X
0 0.2 0.4 0.6 0.8 1
Y
1.16
0.00

- Zeeman splitting ν_Z << linebreath $\Delta\nu$

SiO masers
J=1-0, 2-1, 3-2 etc. of V=1 mostly.

characteristics: highly (~30%) linearly polarized (w. "reversals")
and significant (5-10%) circular polarization (implying B ~ ten's of Gauss if Zeeman)

---

key issues:

- Do linear polarization "reversals" indicate change in direction of magnetic field?, or what?
- Is the circular polarization due to the Zeeman effect, and hence indicates the strength of the magnetic field?

Benchmarks in this regime are the "classic" analytic results for the linear polarization due to Goldreich, Keeley & Kwan.

"a beam of maser radiation in a magnetic field becomes polarized (linearly)."

Polarization vectors of SiO masers around star

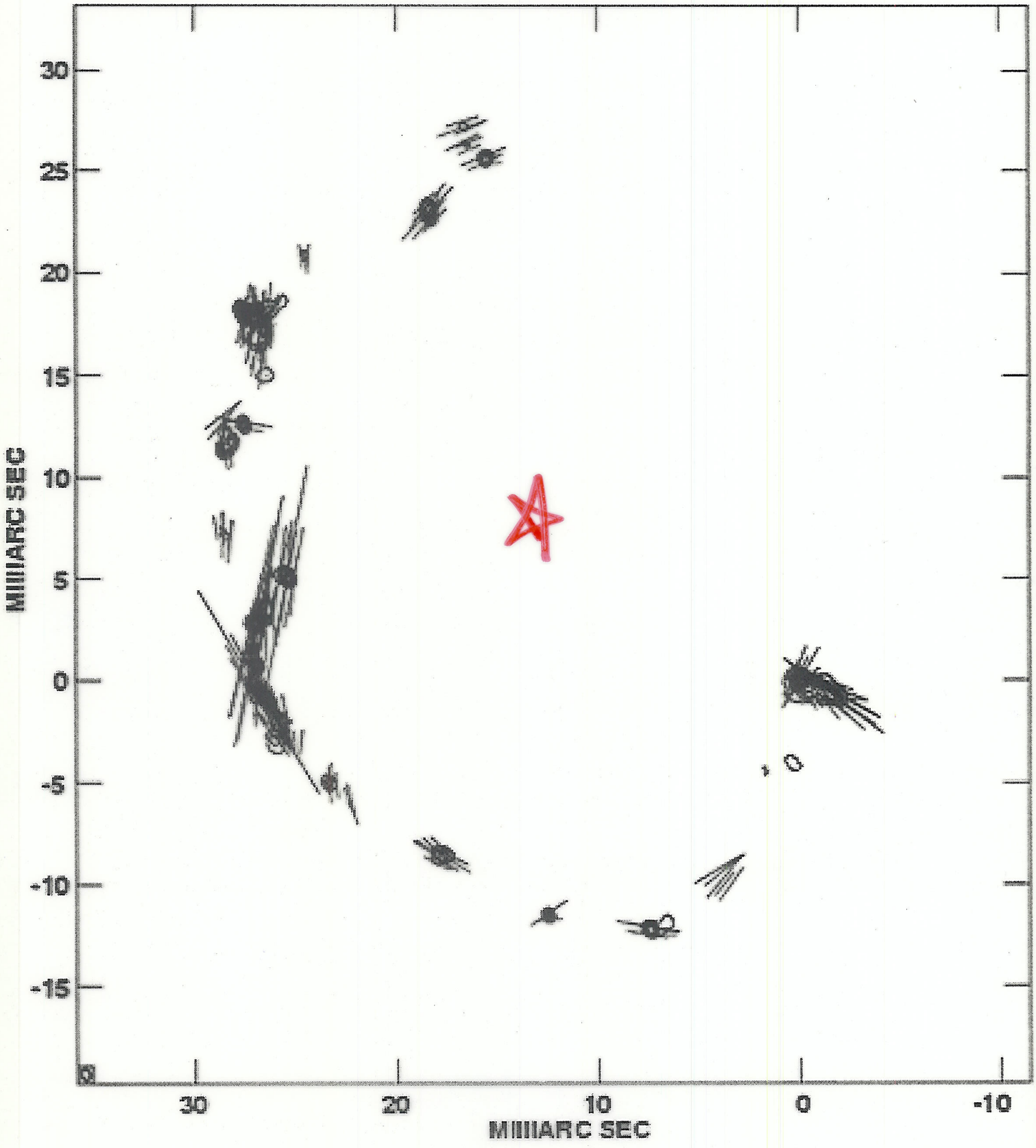

A. Kemball

- General equations simplify greatly
  for $2\pi\nu_z \gg$ lifetime
  for low angular momentum
  for $m \to -m$ symmetry.

(some or all have been made in essentially all calculations)

- More compact and elegant methods (but less transperant?) are available and used in solar physics (e.g. Casini, later today?), but have only been used for masers in a limited calculation (Ramos, Degl'Innocenti + Bueno [2005]).

$J = 1$–0 have not been shown to be representative for maser transitions involving other angular momenta. Examining this issue is a primary goal of the calculation presented here.

In § II, we present the results of reformulating the treatment of polarized maser radiation in the presence of magnetic fields in a way that seems somewhat more convenient for calculations with masing states having angular momenta greater than $J = 1$ and 0. Calculations are then performed for the case of small Zeeman splitting (spectral line breadths $\Delta\omega \gg g\Omega$) (§ III). We emphasize that the idealizations in the physics that are made in performing these calculations are completely equivalent to those made previously (GKK) in calculations for a $J = 1$–0 transition. The qualitative differences in the predicted polarizations are due solely to the higher angular momenta that are considered here. A discussion of the results is presented in § IV. The emphasis is on obtaining asymptotic (with intensity) solutions for the polarization which have served as the benchmarks for the general character of maser radiation generated in the presence of a magnetic field since they were presented by GKK for a $J = 1$–0 transition.

II. BASIC EQUATIONS

Reformulating the calculation for the transfer of polarized maser radiation to provide a systematic treatment of molecular states with various angular momenta is straightforward but tedious. The key generalization from previous work (GKK) is in expressing the matrix elements of the electric dipole operator in terms of angular momentum (Clebsch-Gordon) coefficients by utilizing the Wigner-Eckart Theorem. Only the result is presented here though the detailed manipulations are given in the Appendix. As in previous studies, we approximate the radiative transport as one-dimensional. The maser amplification is expected to favor strongly the maser rays with the longest paths. For propagation of the maser radiation along the z-axis, the equations for radiative transfer of the frequency dependent Stokes parameters $I(\omega)$, $Q(\omega)$, $V(\omega)$, and $U(\omega)$ are

$$\frac{d}{dz}\begin{pmatrix} I(\omega) \\ Q(\omega) \\ U(\omega) \\ V(\omega) \end{pmatrix} = \begin{pmatrix} A & B & F & C \\ B & A & E & G \\ F & -E & A & D \\ C & -G & -D & A \end{pmatrix}\begin{pmatrix} I(\omega) \\ Q(\omega) \\ U(\omega) \\ V(\omega) \end{pmatrix}, \tag{1}$$

where

$$[I, Q, U, V] = \int_0^{+\infty} d\omega[I(\omega), Q(\omega), U(\omega), V(\omega)], \tag{2}$$

for the entire spectral line are obtained by integrating over the profile of the spectral line.

For the elements of the matrix in equation (1) that describes the radiative transfer of the Stokes parameters, we have

$$A(\omega) = (-\pi\omega/c\hbar)\sum_{ab}\int dv\left\{\sum_{b'}\rho_{b'b}(\gamma_+^{ab} + \gamma_-^{ab'})[(d_+^{ab})^* d_+^{ab'} + (d_-^{ab})^* d_-^{ab'}] - \sum_{a'}\rho_{aa'}(\gamma_+^{ab} + \gamma_-^{a'b})[(d_+^{ab})^* d_+^{a'b} + (d_-^{ab})^* d_-^{a'b}]\right\}, \tag{3a}$$

$$B(\omega) = (\pi\omega/c\hbar)\sum_{ab}\int dv\left\{\sum_{b'}\rho_{b'b}(\gamma_+^{ab} + \gamma_-^{ab'})[(d_+^{ab})^* d_-^{ab'} + (d_-^{ab})^* d_+^{ab'}] - \sum_{a'}\rho_{aa'}(\gamma_+^{ab} + \gamma_-^{a'b})[(d_+^{ab})^* d_-^{a'b} + (d_-^{ab})^* d_+^{a'b}]\right\}, \tag{3b}$$

$$C(\omega) = (-\pi\omega/c\hbar)\sum_{ab}\int dv\left\{\sum_{b'}\rho_{b'b}(\gamma_+^{ab} + \gamma_-^{ab'})[(d_+^{ab})^* d_+^{ab'} - (d_-^{ab})^* d_-^{ab'}] - \sum_{a'}\rho_{aa'}(\gamma_+^{ab} + \gamma_-^{a'b})[(d_+^{ab})^* d_+^{a'b} - (d_-^{ab})^* d_-^{a'b}]\right\}, \tag{3c}$$

$$D(\omega) = (-i\pi\omega/c\hbar)\sum_{ab}\int dv\left\{\sum_{b'}\rho_{b'b}(\gamma_+^{ab} - \gamma_-^{ab'})[(d_+^{ab})^* d_-^{ab'} + (d_-^{ab})^* d_+^{ab'}] - \sum_{a'}\rho_{aa'}(\gamma_+^{ab} - \gamma_-^{a'b})[(d_+^{ab})^* d_-^{a'b} + (d_-^{ab})^* d_+^{a'b}]\right\}, \tag{3d}$$

$$E(\omega) = (i\pi\omega/c\hbar)\sum_{ab}\int dv\left\{\sum_{b'}\rho_{b'b}(\gamma_+^{ab} - \gamma_-^{ab'})[(d_+^{ab})^* d_+^{ab'} - (d_-^{ab})^* d_-^{ab'}] - \sum_{a'}\rho_{aa'}(\gamma_+^{ab} - \gamma_-^{a'b})[(d_+^{ab})^* d_+^{a'b} - (d_-^{ab})^* d_-^{a'b}]\right\}, \tag{3e}$$

$$F(\omega) = (i\pi\omega/c\hbar)\sum_{ab}\int dv\left\{\sum_{b'}\rho_{b'b}(\gamma_+^{ab} + \gamma_-^{ab'})[(d_+^{ab})^* d_-^{ab'} - (d_-^{ab})^* d_+^{ab'}] - \sum_{a'}\rho_{aa'}(\gamma_+^{ab} + \gamma_-^{a'b})[(d_+^{ab})^* d_-^{a'b} - (d_-^{ab})^* d_+^{a'b}]\right\}, \tag{3f}$$

$$G(\omega) = (-\pi\omega/c\hbar)\sum_{ab}\int dv\left\{\sum_{b'}\rho_{b'b}(\gamma_+^{ab} - \gamma_-^{ab'})[(d_+^{ab})^* d_-^{ab'} - (d_-^{ab})^* d_+^{ab'}] - \sum_{a'}\rho_{aa'}(\gamma_+^{ab} - \gamma_-^{a'b})[(d_+^{ab})^* d_-^{a'b} - (d_-^{ab})^* d_+^{a'b}]\right\}. \tag{3g}$$

The indices a, a' and b, b' designate the various magnetic substates of the upper and lower molecular states, respectively, of the maser transition. Frequency variations are expressed by the

$$\gamma_\pm^{ab} \equiv \gamma_\pm^{ab}(\omega, v) \equiv \left\{\Gamma \pm i\left[\omega_{ab} - \omega\left(1 - \frac{v}{c}\right)\right]\right\}^{-1}, \tag{4}$$

where $\hbar\omega_{ab}$ is the energy difference between states a and b (including Zeeman splittings), and v is the component of the molecular velocity along the direction of propagation. The ρ_{ij} (see Appendix) are elements of the density matrix for the molecular states. Matrix elements $d_\pm^{ab}$ are obtained by evaluating the dipole moment operator

$$\bar{d} = q\bar{r} = \sum_{p=\pm 1}(-1)^p d_p \hat{e}_p, \tag{5}$$

where $\bar{r}$ is the position operator, q is the charge, and $\hat{e}_p$ are unit vectors for the two helicities relative to the direction of propagation. Hence

$$d_p^{ab} \equiv \langle a | d_p | b \rangle. \tag{6}$$

Equations (1) and (3a)–(3g) together with equations (A39) and (A40) are the basic equations to be solved. They are even more complicated than they appear, since the pumping rates [$\lambda_i \equiv \lambda_i(v)$ in the Appendix], the resonance profiles $\gamma_\pm^{ij} \equiv \gamma_\pm^{ij}(\omega, v)$, and the elements of the density matrix $\rho_{ij} \equiv \rho_{ij}(v)$ are functions of velocity; $\gamma_\pm^{ij}$ is a function of frequency as well.

III. LIMITING POLARIZATION FOR SMALL ZEEMAN SPLITTING

In the limit in which the characteristic Zeeman splitting $g\Omega$ is much less than the spectral line breadth $\Delta\omega$, the Zeeman splitting can be ignored in the resonance profile $\gamma_\pm^{ij}$ while it is retained in the frequencies $\omega_{aa'}$ and $\omega_{bb'}$ that appear in equations (A39) and (A40). In this regime there is only linear polarization, since nothing is present to break the right/left circular

but greatly simplified for Zeeman splitting ≫ lifetime

equations and recognize that the amplitudes $\mathscr{E}_p(s,t)$ and $\mathscr{P}_p(s,t)$ expressed as a function of the distance s along the direction of propagation (the z'-axis) and defined by

$$E_p(s,t) = \mathscr{E}_p(s,t)\exp\left[-i\omega_0(t-s/c)\right], \tag{A15}$$

and

$$P_p(s,t) = \mathscr{P}_p(s,t)\exp\left[-i\omega_0(t-s/c)\right], \tag{A16}$$

are slowly varying in space and time. This yields (see GKK)

$$\left(\frac{1}{c}\frac{\partial}{\partial t}+\frac{\partial}{\partial s}\right)\mathscr{E}_p(s,t) = \frac{2\pi i\omega_0}{c}\mathscr{P}_p(s,t), \tag{A17}$$

and then

$$\left(\frac{1}{c}\frac{\partial}{\partial t}+\frac{\partial}{\partial s}\right)[\mathscr{E}_p(\mathscr{E}_{p'})^*] = \frac{2\pi i\omega_0}{c}[\mathscr{P}_p(\mathscr{E}_{p'})^* - (\mathscr{P}_{p'})^*\mathscr{E}_p]. \tag{A18}$$

The polarization properties of the radiation can be expressed in terms of the (real) Stokes parameters

$$I = \frac{c}{8\pi}(\langle\mathscr{E}_-\mathscr{E}_-^*\rangle + \langle\mathscr{E}_+\mathscr{E}_+^*\rangle), \tag{A19}$$

$$V = \frac{c}{8\pi}(\langle\mathscr{E}_-\mathscr{E}_-^*\rangle - \langle\mathscr{E}_+\mathscr{E}_+^*\rangle), \tag{A20}$$

and

$$Q - iU = -\frac{c}{4\pi}\langle\mathscr{E}_-\mathscr{E}_+^*\rangle, \tag{A21}$$

where the angle brackets indicate time averages over the fluctuations of the system.

In order to examine the spectral dependence of the radiation, express the electric field as a Fourier integral

$$E_p(s,t) = \frac{1}{\sqrt{2\pi}}\int_{-\infty}^{+\infty} E_p(\omega)e^{-i\omega(t-s/c)}\,d\omega. \tag{A22}$$

The assumption of a stationary system implies that the time averages,

$$\langle E_p(\omega)E_{p'}^*(\omega')\rangle = 2\pi F_{pp'}(\omega)\delta(\omega-\omega'). \tag{A23}$$

The polarization of the medium can also be expressed as a Fourier integral of the electric field and of the (yet to be determined) frequency dependent susceptibilities $\chi_{pp'}(\omega)$,

$$P_p(s,t) = \sum_{p'}\frac{1}{\sqrt{2\pi}}\int_{-\infty}^{+\infty}\chi_{pp'}(\omega)E_{p'}(\omega)e^{-i\omega(t-s/c)}\,d\omega. \tag{A24}$$

Inserting equations (A22)–(A24) into equation (A18) along with equations (A15) and (A19)–(A21) yields the radiative transfer equation (1) for the frequency-dependent Stokes parameters $I(\omega)$, $Q(\omega)$, $V(\omega)$, and $U(\omega)$.

In arriving at equation (1), we have ignored the fluctuations in $\chi_{pp'}(\omega)$ in obtaining the time averages. This will be discussed subsequently in solving the equation of motion for the density matrix. The elements A–G of the matrix are dependent on frequency,

$$A = (i\pi\omega/c)(\chi_{++} - \chi_{++}^* + \chi_{--} - \chi_{--}^*), \tag{A25a}$$

$$B = (i\pi\omega/c)(-\chi_{+-} + \chi_{+-}^* - \chi_{-+} + \chi_{-+}^*), \tag{A25b}$$

$$C = (i\pi\omega/c)(-\chi_{++} + \chi_{++}^* + \chi_{--} - \chi_{--}^*), \tag{A25c}$$

$$D = (-\pi\omega/c)(\chi_{+-} + \chi_{+-}^* + \chi_{-+} + \chi_{-+}^*), \tag{A25d}$$

$$E = (-\pi\omega/c)(\chi_{++} + \chi_{++}^* - \chi_{--} - \chi_{--}^*), \tag{A25e}$$

$$F = (-\pi\omega/c)(\chi_{+-} + \chi_{+-}^* - \chi_{-+} - \chi_{-+}^*), \tag{A25f}$$

and

$$G = (i\pi\omega/c)(-\chi_{+-} + \chi_{+-}^* + \chi_{-+} - \chi_{-+}^*). \tag{A25g}$$

The matrix elements A–G thus are real.

The polarizations and hence the susceptibilities are determined from the elements of the density matrix ρ for the molecular states. These matrix elements are obtained by solving the equation of motion for the density matrix,

$$\frac{\partial\rho}{\partial t} = -(i/\hbar)(H\rho - \rho H) - \Gamma\rho + \Lambda, \tag{A26}$$

d as time independent,

$$\dot{\rho}_{aa'} = \frac{\partial \rho_{aa'}}{\partial t} = \gamma_a \delta_{aa'} - (\Gamma + i\omega_{aa'})\rho_{aa'} - (i/\hbar) \sum_b (V_{ab}\rho_{ba'} - \rho_{ab} V_{ba'}) . \tag{A36}$$

the λ_a (and λ_b) are the elements of the diagonal pumping matrix Λ and the $\omega_{aa'}$ (and $\omega_{bb'}$) are the energy differences $(E_a - E_{a'})/\hbar$ $[E_b - E_{b'}]/\hbar$) due to the interaction with the static magnetic field. The equations for the $\partial\rho_{bb'}/\partial t$ are exactly analogous to ion (A36).

om equations (A22), (A23), (A27), and (A33), the time averages of the terms in equation (A36) can be evaluated,

$$\langle V_{ab}\rho_{ba'}\rangle = (i/4\hbar) \sum_p d^{ab}_{-p} \sum_{p'} \left[\sum_{b'} (d^{a'b'}_{-p'}\rho_{b'b})^* - \sum_{a''} (\rho_{a'a''} d^{a''b}_{-p'})^* \right] \int F_{pp'}(\omega)\gamma^{a'b}_{-} d\omega . \tag{A37}$$

e is a similar equation for $\langle \rho_{ab} V_{ba'}\rangle$. Substituting these into equation (A36) yields

$$\begin{aligned} 0 = {} & \lambda_a \delta_{aa'} - (\Gamma + i\omega_{aa'})\rho_{aa'} \\ & + (1/4\hbar^2) \sum_b \sum_p d^{ab}_{-p} \sum_{p'} \left[\sum_{b'} (d^{a'b'}_{-p'}\rho_{b'b})^* - \sum_{a''} (\rho_{a'a''} d^{a''b}_{-p'})^* \right] \int F_{pp'}(\omega)\gamma^{a'b}_{-} d\omega \\ & + (1/4\hbar^2) \sum_b \sum_p (d^{a'b}_{-p})^* \sum_{p'} \left(\sum_{b'} d^{ab'}_{-p'}\rho_{b'b} - \sum_{a''} \rho_{aa''} d^{a''b}_{-p'} \right) \int F_{p'p}(\omega)\gamma^{ab}_{+} d\omega \end{aligned} \tag{A38}$$

nilar equation holds for $\rho_{bb'}$.

terms of the Stokes parameters, equation (A38) becomes

$$\begin{aligned} \dot{\rho}_{aa'} = {} & \lambda_a \delta_{aa'} - (\Gamma + i\omega_{aa'})\rho_{aa'} + (\pi/c\hbar^2) \sum_{bb'} \rho_{b'b} \int d\omega\, (\gamma^{a'b'}_{-} + \gamma^{ab}_{+})\{I(\omega)[(d^{a'b}_{+})^* d^{ab'}_{+} + (d^{a'b}_{-})^* d^{ab'}_{-}] - Q(\omega)[(d^{a'b}_{+})^* d^{ab'}_{-} + (d^{a'b}_{-})^* d^{ab'}_{+}] \\ & - iU(\omega)[(d^{a'b}_{+})^* d^{ab'}_{-} - (d^{a'b}_{-})^* d^{ab'}_{+}] + V(\omega)[(d^{a'b}_{+})^* d^{ab'}_{+} - (d^{a'b}_{-})^* d^{ab'}_{-}]\} - (\pi/c\hbar^2) \sum_{ba''} \rho_{a''a'} \int d\omega\, \gamma^{a'b}_{-}\{I(\omega)[d^{ab}_{+}(d^{a''b}_{+})^* + d^{ab}_{-}(d^{a''b}_{-})^*] \\ & - Q(\omega)[d^{ab}_{+}(d^{a''b}_{-})^* + d^{ab}_{-}(d^{a''b}_{+})^*] + iU(\omega)[d^{ab}_{+}(d^{a''b}_{-})^* - d^{ab}_{-}(d^{a''b}_{+})^*] + V(\omega)[d^{ab}_{+}(d^{a''b}_{+})^* - d^{ab}_{-}(d^{a''b}_{-})^*]\} \\ & - (\pi/c\hbar^2) \sum_{ba''} \rho_{aa''} \int d\omega\, \gamma^{ab}_{+}\{I(\omega)[(d^{a'b}_{+})^* d^{a''b}_{+} + (d^{a'b}_{-})^* d^{a''b}_{-}] - Q(\omega)[(d^{a'b}_{+})^* d^{a''b}_{-} + (d^{a'b}_{-})^* d^{a''b}_{+}] \\ & - iU(\omega)[(d^{a'b}_{+})^* d^{a''b}_{-} - (d^{a'b}_{-})^* d^{a''b}_{+}] + V(\omega)[(d^{a'b}_{+})^* d^{a''b}_{+} - (d^{a'b}_{-})^* d^{a''b}_{-}]\} . \end{aligned} \tag{A39}$$

: analogous equation for the lower state is

$$\begin{aligned} 0 = {} & \lambda_b \delta_{bb'} - (\Gamma_b + i\omega_{bb'})\rho_{bb'} + (\pi/c\hbar^2) \sum_{aa'} \rho_{a'a} \int d\omega\, (\gamma^{a'b'}_{+} + \gamma^{ab}_{-})\{I(\omega)[(d^{a'b}_{+})^* d^{ab'}_{+} + (d^{a'b}_{-})^* d^{ab'}_{-}] - Q(\omega)[(d^{a'b}_{+})^* d^{ab'}_{-} + (d^{a'b}_{-})^* d^{ab'}_{+}] \\ & - iU(\omega)[(d^{a'b}_{+})^* d^{ab'}_{-} - (d^{a'b}_{-})^* d^{ab'}_{+}] + V(\omega)[(d^{a'b}_{+})^* d^{ab'}_{+} - (d^{a'b}_{-})^* d^{ab'}_{-}] - (\pi/c\hbar^2) \sum_{ab''} \rho_{b''b'} \int d\omega\, \gamma^{ab'}_{+}\{I(\omega)[(d^{ab}_{+})^* d^{ab''}_{+} + (d^{ab}_{-})^* d^{ab''}_{-}] \\ & - Q(\omega)[(d^{ab}_{+})^* d^{ab''}_{-} + (d^{ab}_{-})^* d^{ab''}_{+}] - iU(\omega)[(d^{ab}_{+})^* d^{ab''}_{-} - (d^{ab}_{-})^* d^{ab''}_{+}] + V(\omega)[(d^{ab}_{+})^* d^{ab''}_{+} - (d^{ab}_{-})^* d^{ab''}_{-}] \\ & - (\pi/c\hbar^2) \sum_{ab''} \rho_{bb''} \int d\omega\, \gamma^{ab}_{-}\{I(\omega)[(d^{ab''}_{+})^* d^{ab'}_{+} + (d^{ab''}_{-})^* d^{ab'}_{-}] - Q(\omega)[(d^{ab''}_{+})^* d^{ab'}_{-} + (d^{ab''}_{-})^* d^{ab'}_{+}] \\ & - iU(\omega)[(d^{ab''}_{+})^* d^{ab'}_{-} - (d^{ab''}_{-})^* d^{ab'}_{+}] + V(\omega)[(d^{ab''}_{+})^* d^{ab'}_{+} - (d^{ab''}_{-})^* d^{ab'}_{-}] . \end{aligned} \tag{A40}$$

REFERENCES

raham, Z., Cohen, N. L., Opher, R., Raffaelli, J. C., and Zisk, S. H. 1981, *Astr. Ap.*, **100**, L10.
rvainis, R. E., and Deguchi, S. 1989, *A.J.*, **97**, 1089.
rvainis, R. E., McIntosh, G., and Predmore, C. R. 1987, *Nature*, **329**, 613.
logna, J. M., Johnston, K. J., Knowles, S. H., Mango, S. A., and Sloanaker, R. M. 1975, *Ap. J.*, **199**, 86.
hen, P. J., Downs, G., Emerson, R., Grimm, M., Stevens, G., and Tarter, J. 1987, *M.N.R.A.S.*, **225**, 491.
guchi, S., and Watson, W. D. 1986, *Ap. J.*, **302**, 750.
guchi, S., Watson, W. D., and Western, L. R. 1986, *Ap. J.*, **302**, 108.
wnes, D. 1985, in *Proc. Les Houches Summer School (Session XLI)*, ed. R. Lucas, A. Omont, and R. Stora (Amsterdam: North Holland), p. 557.
lmonds, A. R. 1968, *Angular Momentum in Quantum Mechanics* (Princeton: Princeton University Press).
itzur, M., Hollenbach, D., and McKee, C. F. 1989, *Ap. J.*, **346**, 983.
Fiebig, D., and Gusten, R. 1989, *Astr. Ap.*, **214**, 333.
Fix, J. D. 1987, *A.J.*, **93**, 433.
Garay, G., Moran, J. M., and Haschick, A. D. 1989, *Ap. J.*, **338**, 244.
Garcia-Barretto, J. A., Burke, B. F., Reid, M. J., Moran, J. M., Haschick, A. D., and Schilizzi, R. T. 1988, *Ap. J.*, **326**, 954.
Genzel, R. 1986, in *Masers, Molecules and Mass Outflows in Star Forming Regions*, ed. A. D. Haschick (Westford, MA: Haystack Observatory), p. 233.
Goldreich, P., Keeley, D. A., and Kwan, J. Y. 1973, *Ap. J.*, **179**, 111 (GKK).
Gwinn, C. R., Moran, J. M., Reid, M. J., and Schneps, M. H. 1988, *Ap. J.*, **330**, 817.
Knowles, S. H., and Batchelor, R. A. 1978, *M.N.R.A.S.*, **194**, 107.
Kylafis, N. D., and Norman, C. 1987, *Ap. J.*, **323**, 346.
Matveenko, L. I., Graham, D. A., and Diamond, P. J. 1988, *Soviet Astr. Letters*, **6**, 468.
McIntosh, G. 1987, Ph.D. dissertation, University of Massachusetts.

Some results from numerically integrating polarized equations for a linear maser

- modifications to stokes V due to "simple" radiative saturation ($2\pi \nu_z >>$ lifetime)
- Creating "non-Zeeman" Stokes V from Stokes Q, U caused by irregular magnetic fields which change direction.
- creating "non-Zeeman" Stokes V when $2\pi \nu_z \simeq$ lifetime.

Polarization of Maser Radiation (constant magnetic field)

Zeeman (weak splitting)

"Circular polarization"

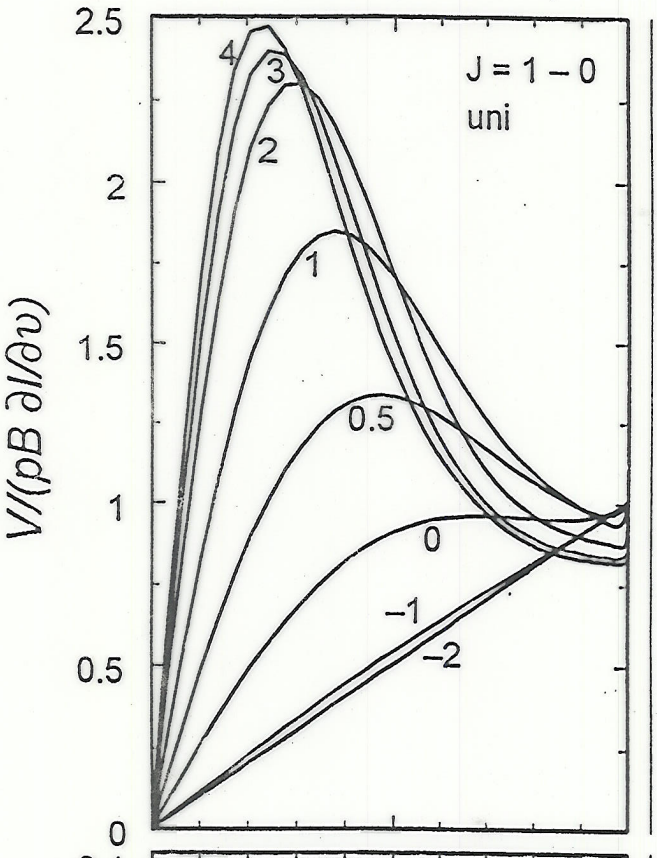

linear polarization

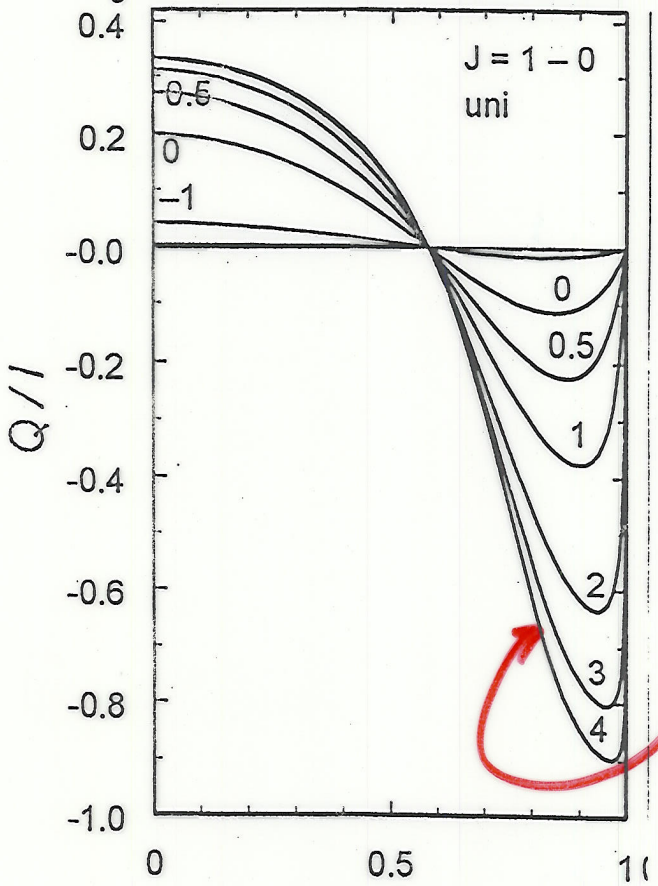

Goldreich, Keeley, Kwan "classic result"

Watson + Wyld 2001

Maser radiation from a turbulent medium

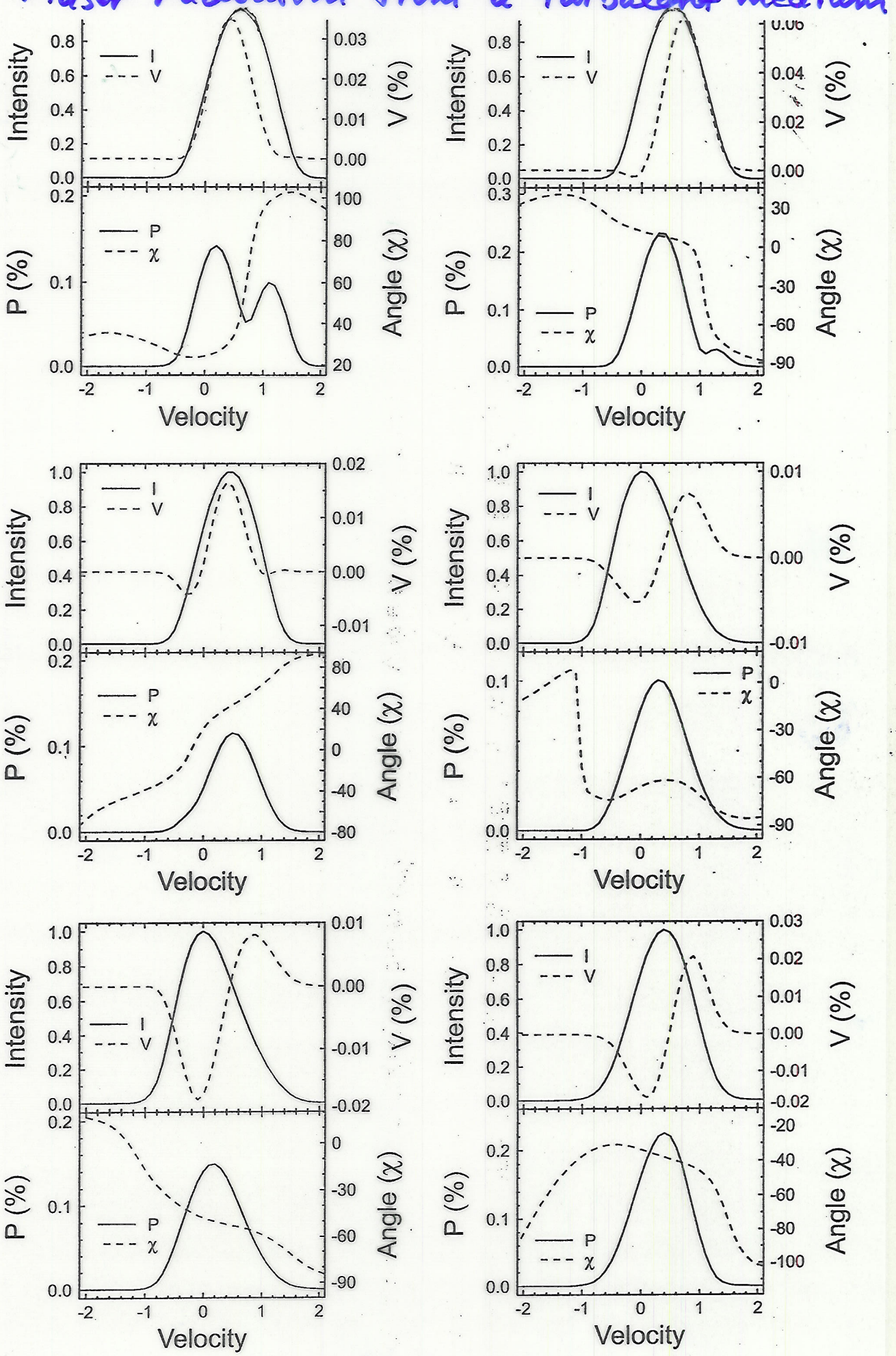

V = "non-Zeeman" Stokes-V

Wiebe & Watson